



ELSEVIER

Available online at www.sciencedirect.com

ScienceDirect

journal homepage: www.intl.elsevierhealth.com/journals/dema

Adherence of oral streptococci to nanostructured titanium surfaces

Krunal Narendrakumar^{a,1}, Mukta Kulkarni^{b,1}, Owen Addison^a,
Anca Mazare^c, Ita Junkar^d, Patrik Schmuki^c, Rachel Sammons^{a,*},
Aleš Iglič^b

^a School of Dentistry, University of Birmingham, St Chad's Queensway, Birmingham B4 6NN, UK

^b Laboratory of Biophysics, Faculty of Electrical Engineering, University of Ljubljana, Ljubljana SI-1000, Slovenia

^c Department of Materials Science and Engineering, Chair of Surface Science and Corrosion,
University of Erlangen–Nuremberg, WW4-LKO, Erlangen, Germany

^d Jožef Stefan Institute, Jamova cesta 39, Ljubljana SI-1000, Slovenia

ARTICLE INFO

Article history:

Received 23 May 2015

Received in revised form

15 July 2015

Accepted 21 September 2015

Available online xxx

Keywords:

TiO₂

Anodization

Nanotexture

Dental implant

Antimicrobial

Peri-implantitis

ABSTRACT

Objectives. Peri-implantitis and peri-mucositis pose a severe threat to the success of dental implants. Current research focuses on the development of surfaces that inhibit biofilm formation while not interfering with tissue integration. This study compared the adherence of two oral bacterial species, *Streptococcus sanguinis* and *Streptococcus mutans* to nanostructured titanium surfaces.

Methods. The samples included TiO₂ nanotubes formed by anodization of titanium foil of 100, 50 and 15 nm diameter (NT15, NT50, NT100), a nanoporous (15 nm pore diameter) surface and compact TiO₂ control. Adherent surviving bacteria were enumerated after 1 h in an artificial saliva medium containing bovine mucin.

Results. Lowest numbers of adherent bacteria of both species were recovered from the original titanium foil and nanoporous surface and highest numbers from the Ti100 nanotubes. Numbers of attached *S. sanguinis* increased in the order (NT15 < NT50 < NT100), correlated with increasing percentage of surface fluoride. The lowest adhesion of *S. sanguinis* and *S. mutans* on TiO₂ nanostructured surfaces was observed for small diameter nanoporous surfaces which coincides with the highest osteoblast adhesion on small diameter nanotubular/nanoporous surfaces shown in previous work.

Significance. This study indicates that the adherence of oral streptococci can be modified by titanium anodization and nanotube diameter.

© 2015 Academy of Dental Materials. Published by Elsevier Ltd. All rights reserved.

* Corresponding author. Tel.: +44 121 466 5539; fax: +44 121 466 5542.

E-mail address: r.l.sammons@bham.ac.uk (R. Sammons).

¹ Equally share the first authorship.

<http://dx.doi.org/10.1016/j.dental.2015.09.011>

0109-5641/© 2015 Academy of Dental Materials. Published by Elsevier Ltd. All rights reserved.

1. Introduction

The reported success rates of dental implants are high when considered solely in terms of initial implant osseointegration, however there is unpredictability in the initial generation and subsequent stability of the peri-implant soft tissue architecture over the lifetime of the implant [1]. The adherence and proliferation of potentially pathogenic bacteria on Ti implant surfaces has been directly linked to the peri-implant inflammatory changes which occur and may be limited to the soft-tissues (mucositis) or associated with progressive loss of osseointegration (peri-implantitis) [2]. The results of a review of the frequency of peri-implant diseases involving a meta-analysis of 504 studies with 1497 participants and 6283 implants suggested that 63.4% of the participants and 30.7% of implants suffered from peri-implant mucositis and 18.8% participants and 9.6% of implants were affected by peri-implantitis [3]. As the number of dental implants increases in the population, peri-implant disease is likely to become a particularly significant burden for patients and healthcare providers alike. This is of particular significance in the elderly where a loss of manual dexterity and a decreased salivary flow predisposes to poor hygiene around dental implant fixtures leading to an increased risk of peri-implant disease [1]. Consequently, contemporary research is focusing on the development of surfaces to facilitate osseointegration [4,5], as well as to support the formation of a healthy cuff of keratinized mucosa around the implant abutment, providing a barrier to prevent the passage of microorganisms into the underlying connective tissues [6–8].

Nanotexturing is being widely explored as a means of encouraging cellular attachment and techniques include the incorporation of nanoparticulates and modification of nanoscale surface topography to encourage cell adhesion and inhibit bacterial attachment and biofilm formation [8–11].

In the past, several methods have been developed to produce nanoscale structures on Ti surfaces and electrochemical anodization of Ti is a powerful tool to control nanoscale architecture for surface modification. To improve the biological, chemical, and mechanical properties of the biomaterial, significant research has been carried out to find more suitable topologies which could present improved bioperformance (reviewed by Kulkarni et al. [12]). Titanium dioxide (TiO₂) nanotubes can be easily synthesized by electrochemical anodization of Ti using a two electrode electrochemical cell, and the electrochemical formation of self-organized TiO₂ nanotubes layers in dilute fluoride containing electrolytes has been studied intensively [13–16]. It was shown that the water content in the electrolyte is the critical factor that determines whether self-ordered oxide nanotubes or nanopores are formed during the electrochemical anodization, and it is thought that tube formation originates from ordered porous oxide by a “pore-wall-splitting” mechanism [17]. By tailoring the anodization parameters (applied voltage, anodization time and concentrations of chemicals) TiO₂ nanotubes of different diameters from 15 nm to 300 nm and different lengths can be obtained [18,19]. Osteoblast adhesion to TiO₂ nanotubes has been shown to be dependent on tube diameter [20,21]. Peng et al. [22] found that osteoblast adhesion was enhanced, and

Staphylococcus epidermidis adhesion and proliferation reduced on 80 nm compared with 30 nm diameter TiO₂ tubules and smooth controls. They concluded that the effect was due to a combination of surface chemistry (fluorine content), surface roughness and wettability. Gongadze, et al. [20,23] similarly reported that osteoblasts adhered better to 15 nm diameter nanopores/nanotubes than 100 nm diameter nanotubes [12]. However, the effect of such surface modifications on attachment of oral bacteria has not been reported. In the present work, the effect of different nanostructured Ti surface on the adherence of two oral Streptococcal species, *S. sanguinis* and *Streptococcus mutans* that coexist in oral biofilms was investigated. *S. sanguinis* is a primary colonizer of oral plaque and although *S. mutans* is primarily associated with dental caries, both species have been identified in association with dental implants [24–27].

2. Materials and methods

2.1. Preparation of Ti nanotextured surfaces

Ti foils of 0.1 mm thickness and 99.6% purity were used for preparation of different nanostructures. Prior to two-step anodization, Ti foils were degreased by successive ultrasonication in acetone, ethanol and deionized (DI) water for 5 min each and dried in a nitrogen stream. The two-steps anodization (leading to a pre-patterning of the surface) was carried out to achieve nanostructures with higher uniformity and less defects (as a result of using the pre-patterned substrate in the second anodization). All anodization experiments were performed at room temperature, in a two-electrode system with Ti foil as the anode and platinum gauze as the cathode, with a working distance of 15 mm. Briefly, in the first step, Ti foils were anodized in ethylene glycol based electrolyte with 1 M H₂O and 0.1 M NH₄F at 35 V for 2 h. Nanotubes grown in this first step were removed by ultrasonication to get a pre-patterned surface which was then cleaned by successive ultrasonication in acetone and ethanol and used as a substrate for the second step [12]. In the second step, nanostructures were grown in ethylene glycol (EG) based electrolytes containing hydrofluoric (HF) acid and water (H₂O) with specific chemical compositions as shown in Table 1. After the anodization, the nanostructures formed were immersed in ethanol for 2 h to remove all organic components from the electrolyte, washed with distilled water and dried in a nitrogen stream.

2.2. Surface characterization of Ti nanostructures

The morphology of the TiO₂ nanostructures was observed using a field-emission scanning electron microscope – Hitachi FE-SEM S4800 operating at an accelerating voltage of 10.00 kV at 8 mm working distance.

2.3. Atomic Force Microscopy (AFM)

Topographic features of Ti-foil and Ti-nanostructured surfaces were measured by atomic force microscopy (AFM, Solver PRO, NT-MDT, Russia). All the measurements were conducted in tapping mode in air. Samples were scanned with the standard

Table 1 – Anodization conditions used to create the different Ti surface nanostructures (NP: nanopores, NT: nanotubes).

Ti surface/NP/NT diameter	Electrolyte	Potential used	Anodization time
Compact oxide	1 M phosphoric acid	20 V	15 min
NP 15 nm	EG + 6 M water + 0.2 M HF	10 V	1 h
NT 15 nm	EG + 8 M water + 0.2 M HF	10 V	2.5 h
NT 50 nm	EG + 8 M water + 0.2 M HF	20 V	2.5 h
NT 100 nm	EG + 8 M water + 0.2 M HF	58 V	2.5 h

Si cantilever with a force constant of 22 N/m and at a resonance frequency of 325 kHz (using a tip radius of 10 nm and a tip length of 95 μm).

2.4. XPS Analysis of the surfaces

XPS analysis was conducted by Midlands Surface Analysis Ltd, Aston University, Birmingham, in a Thermofisher ESCALAB 250 electron spectrometer equipped with a hemispherical sector energy analyzer. A monochromatic Al $K\alpha$ X-ray source was used for analysis to enhance the resolution. At source excitation energy of 15 KeV, an emission current of 6 mA; an analyzer pass energy of 20 eV with step size of 0.1 eV and a dwell time of 50 ms were used throughout the experiments. The base pressure within the spectrometer during examinations always exceeded 5×10^{-10} mbar, ensuring that all signals recorded were from the sample surface. The area of analysis was 500 μm diameter. XPS survey scans were first recorded for each region examined and then narrow region energy scans were performed for all the elements identified on the surface to determine the chemical state of the specific element identified. To improve statistics, multiple scans were used throughout for all the constituents in the surface.

2.5. Surface wettability

Contact angle measurements were obtained with a Digidrop contact angle meter (GBX, Digidrop Romans Sur Isère, Drôme, France). HPLC grade distilled water ($\gamma = 72.8 \text{ mN m}^{-1}$) 2–2.5 μL droplets were deposited onto each sample surface at room temperature. Contact angles of five drops per sample on 3 samples were analyzed and results are expressed as mean \pm SD of the 15 measurements.

2.6. Bacterial adhesion

A fresh colony of *S. sanguinis* GW2 or *S. mutans* 3209 was used to inoculate 10 ml of artificial saliva [28] and was then incubated with agitation for 24 h in an anaerobic work station (Mini-MAC, Don Whitley Scientific) at 37 °C in an atmosphere of 10% carbon dioxide, 80–85% nitrogen and 5–10% hydrogen for 24 h. Following vortex mixing to disperse aggregates, the suspension was diluted 100 fold in fresh artificial saliva to give approximately 2×10^7 colony forming units (cfu)/ml. Two 5 μL aliquots of the diluted suspension were pipetted onto a sterilized microscope slide enclosed inside a Petri dish to maintain humidity, and the Ti samples to be tested were placed face-down onto the suspension (Fig. 1). The samples were incubated for 1 h in the anaerobic work-station to allow bacterial attachment. Four samples of each Ti surface condition were used for each bacterium. Following incubation

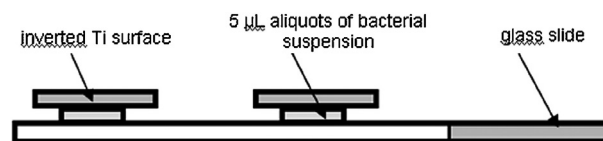


Fig. 1 – The incubation procedure for bacterial adhesion tests. Test surfaces were inverted onto droplets of a bacterial suspension in artificial saliva on microscope slides contained in a Petri dish as shown for 1 h.

the samples were rinsed by immersion in PBS three times to remove loosely bound bacteria. Samples were then placed in separate 7.0 ml bijoux tubes (50 mm \times 20 mm) containing 5 ml of sterile PBS. The containers were then placed in a sonic water bath (Vitasonic, Bad Säckingen, Switzerland) for 10 min, and vortex mixed for 15 s to detach the bacteria that had adhered to the surfaces. 0.1 ml of the sonicated and vortexed sample was plated onto blood agar plates (BioMérieux, Hampshire, UK), and incubated for 24 h in an anaerobic cabinet to obtain colony counts.

2.7. Statistical analysis

Results were analyzed using Analysis of Variance followed by post-hoc Tukey tests for multiple comparisons.

3. Results

3.1. Characterization of Ti nanostructures by SEM and AFM

Specific diameters of TiO_2 nanotubes were obtained by tailoring various anodization parameters such as applied voltage, anodization time and concentrations of chemicals etc. SEM images of the surfaces of the TiO_2 nanostructures are shown in Fig. 2, presenting uniform open-top morphologies with no initiation layer or nanoglass formation [29]. Furthermore, there is a good control over the diameter size; the diameters for the small diameter nanostructures are approximately 13 nm for the nanopores and approximately 16 nm for the nanotubes; here we will refer to these samples as 15 nm nanopores or nanotubes respectively.

AFM demonstrated significant differences in the topography of the prepared Ti surfaces with the pristine Ti foil exhibiting no specific topographic features (Fig. 3a). The nanotubular structures were detectable on the nanostructured surfaces (Fig. 3b and c), however in the case of nanopores and nanotubes of diameters below 50 nm the AFM tip could not reach the inner side of the pore or tube and therefore these structures appeared closed (Fig. 3b). Clear nanotubular

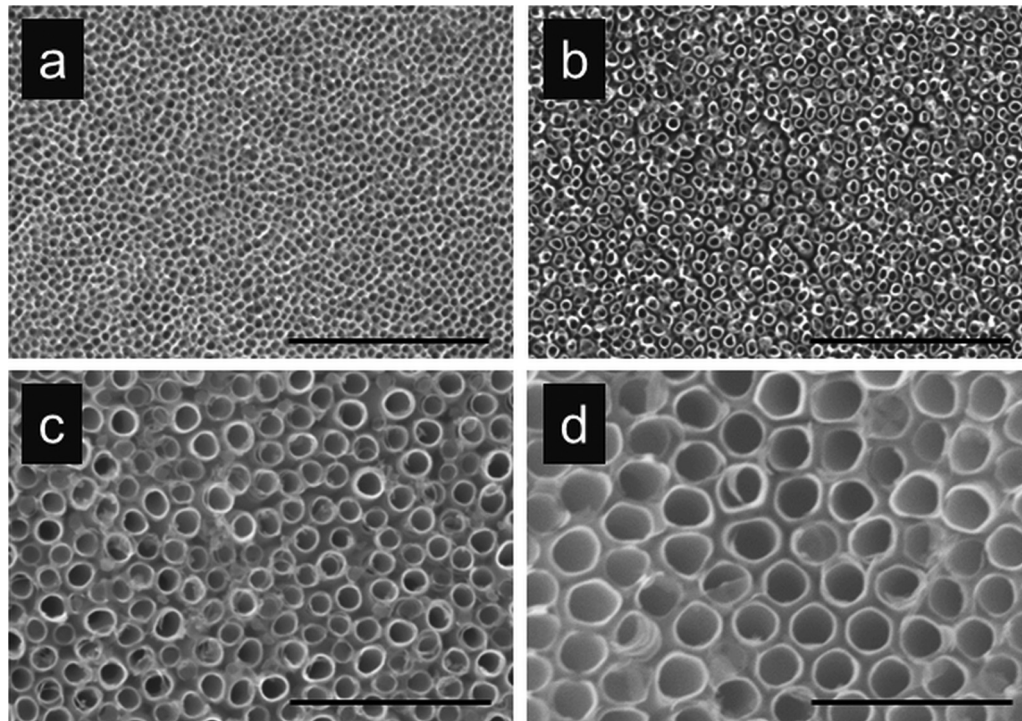


Fig. 2 – SEM images of the upper surface of TiO_2 nanostructures of different diameters: (a) 15 nm NP, (b) 15 nm NT, (c) 50 nm NT, (d) 100 nm NT (NP: nanopores, NT: nanotubes), Scale bar: 500 nm.

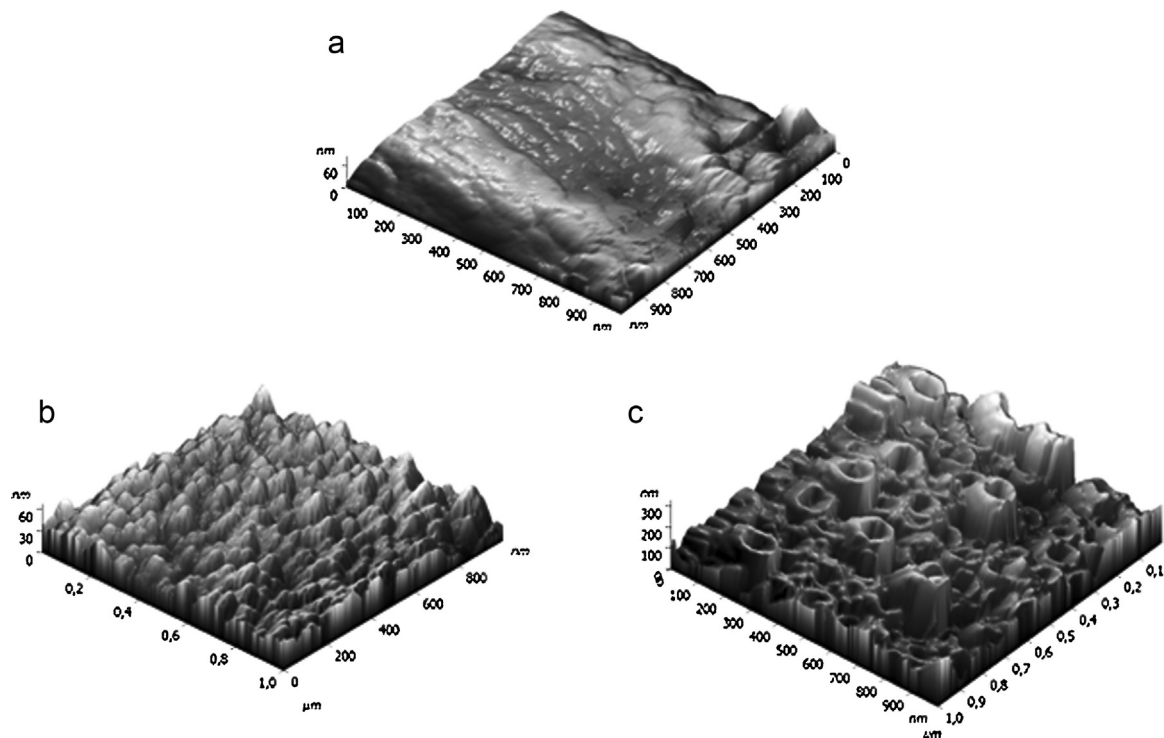


Fig. 3 – AFM Images of Ti-nanostructures: Atomic Force Microscopy images of the (a) pristine Ti foil, (b) the 15 nm diameter nanopore prepared Ti surface and (c) the 100 nm diameter nanotubular surface.

Table 2 – Results of XPS analyses for elemental (atomic) concentration (%) of the nanopore (NP), nanotube (NT), compact oxide (CO) and Ti foil surfaces.

Ti surface/NP/NT diameter	Atomic concentration (%)									F/Ti ratio
	F	Ti	C	O	N	Si	Ca	P	Cl	
NP	1.6	16.5	34.6	45.8	0.7	0.7	–	–	–	0.10
NT15	3.1	15.8	36.2	44.0	0.5	0.4	–	–	–	0.20
NT50	5.8	19.4	24.0	50.2	0.4	0.3	–	–	–	0.30
NT100	7.0	20.4	20.7	51.4	0.5	–	–	–	–	0.34
CO	–	16.4	18.9	57.9	1.7	–	–	5.1	–	–
Ti foil	–	17.9	37.3	40.6	2.5	0.8	0.7	–	0.3	–

structures were observed in the case of the 100 nm nanotube Ti surface (Fig. 3c).

3.2. XPS analysis

Fluorine (F) was detected in the surfaces of the nanoporous and nanotubular samples, increasing in concentration in the order NP→NT15→NT50→NT100. The F was probably in the form of a fluoride (TiF₄) and Ti was present mainly as TiO₂. Nitrogen (N) was detected from a C–N bonded species and silicon (Si) from a silicone, except in sample NT100, where it was absent. In the compact oxide sample (CO), Ti was present mainly as TiO₂, nitrogen as a C–N bonded group and phosphorus (P) as a phosphate (Table 2). Both C–O and O=C–O components consistently increased in the nanotubular samples in the order NT15→NT50→NT100. In the Ti Foil samples there was a substantial carbide component (Table 3), existing as TiC; while N was present as C–N and as a nitride, Si as silicone and Ca as CaCO₃.

3.3. Wettability

Water contact angles were measured on the prepared Ti surfaces (Fig. 4). All the samples were hydrophobic with contact angles >60° and the compact oxide had the lowest contact angle of 60.8±9.0. The nanoporous surface was the most hydrophobic, with a contact angle of 120±1.0, followed by the nanotubular surfaces: NT 15>NT 50>NT100. Only NT100 was slightly more hydrophilic than Ti foil.

3.4. Bacterial adhesion

Adherence of *S. sanguinis* and *S. mutans* on TiO₂ nanostructures is shown in Figs. 5 and 6. Lowest numbers of cfu of both species were recovered from the original titanium

foil and the nanoporous surface and highest numbers from the NT100 nanotubes. In the case of *S. sanguinis* numbers of cfu on the nanotubular arrays decreased in the order NT100>NT50>NT15, with significantly higher numbers recovered from NT100 in comparison with NT50 ($P<0.01$) and NT15 ($P<0.05$) (Fig. 5). The pattern was similar with *S. mutans*, in that the NT100 surface showed the highest level of attachment and in this case equal numbers of cfu were recovered from NT15 and NT50 and similar numbers from the original foil, compact oxide and nanoporous surfaces (Fig. 6).

4. Discussion

Dental implants have been specifically designed to either have roughened surfaces to encourage cellular (mainly osteoblast) interactions or smooth surfaces to facilitate cleaning measures. However surface roughening also increases the surface area available for microbial attachment. From a systemic review of 24 papers Teughels et al. [30] found a clear relationship between increasing surface roughness and plaque formation and concluded that on rough surfaces bacteria are better protected against displacing shear forces and as a result biofilms are able to mature. Furthermore the undisturbed plaques on the rough surfaces were able to harbor more complex biofilms consisting of rods, motile organisms and spirochetes [2].

Previous reports have shown that Ti nanostructured surfaces containing specific topographies can promote the adhesion and differentiation of osteoblasts and other types of eukaryotic cells while suppressing or promoting the adhesion of bacteria [31]. Experiments with anodized samples with 15 and 100 nm diameter nanotubular surfaces, similar morphologies with the samples used in the current study demonstrated that more osteoblasts adhered to 15 nm diameter nanotubes than to 100 nm ones [23,32–34]. A nanotube

Table 3 – Results of XPS analyses for C components (%) of the nanopore (NP), nanotube (NT), compact oxide and Ti foil surfaces.

Ti surface/NP/NT diameter	Atomic %				
	C–C	C–O	O–C–O	C–N	Carbide
NP	78.1	14.6	5.2	2.2	–
NT15	81.6	11.7	4.9	1.8	–
NT50	74.1	18.1	6.1	1.7	–
NT100	61.0	29.2	7.1	2.8	–
CO	66.1	12.7	12.2	9.0	–
Ti foil	64.9	6.0	5.0	3.0	21.1

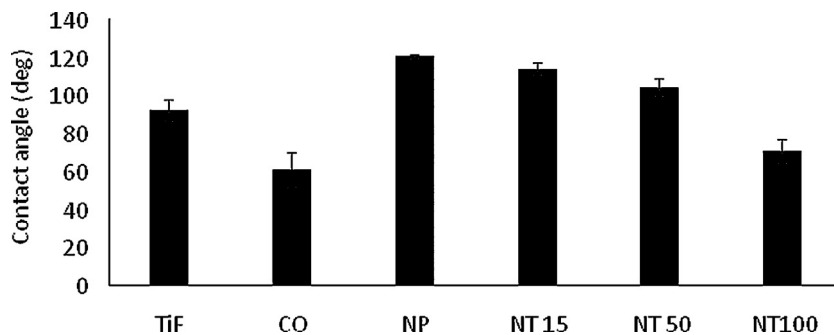


Fig. 4 – Mean water contact angles and associated standard deviations obtained on the nanopore (NP), compact oxide (CO) and Ti foil (TiF) and nanotube (NT) surfaces ($n = 15$). All results were significantly different from each other ($p < 0.05$).

diameter of 15–30 nm seemed to favor adhesion of mammalian cells of several different kinds including mesenchymal stem cells, osteoblasts and osteoclasts, and it was suggested that this may reflect optimal 10 nm clustering of integrins on a surface with this spacing [34]. It is becoming clear that in terms of attachment, the size of the bacteria and mammalian cells in relation to the dimensions of pits, pores and crevasses in the surface is important, as well as differences in surface energy and composition. The formation of a proteinaceous conditioning film may mask some topographical features but protein adsorption is itself governed by physicochemical properties and the proteins may present functional groups that enhance or inhibit attachment (reviewed by Neoh et al. [5]).

Here we have shown that in the presence of artificial saliva, which contains the protein mucin as a component, anodization actually appeared to increase adhesion compared with the original titanium foil but on the anodized nanotubular surfaces more streptococci of both species adhered to the 100 nm diameter nanotubes than to those of smaller diameter and to the 15 nm nanoporous surface. This is in contrast to other

studies with staphylococci on somewhat similar surfaces but in different medium. For example, Peng et al. [22] demonstrated that *Staphylococcus epidermidis* adhesion was reduced on 80 nm diameter nanotubes in comparison with 30 nm ones, while, in contrast, the adherence of osteoblast-like cells was enhanced on the 80 nm nanotubular surface. Pucket et al. [35] demonstrated that certain Ti surfaces with nanometer sized features could promote osteoblast adhesion while reducing attachment of staphylococcal and pseudomonas bacteria in comparison with a conventional Ti surface over a 1 h attachment period.

The reasons for the observed differences in streptococcal attachment are currently not clear. Streptococci employ a great variety of adhesion mechanisms and both species of streptococci adhere to mucin components. It has recently been shown that the 100 nm nanotubes have the highest surface area and capacity for serum protein adsorption [36] and this could be an important influence on both bacterial and cell attachment meriting further investigation. Adherence of both Gram negative and Gram positive bacteria has been shown to

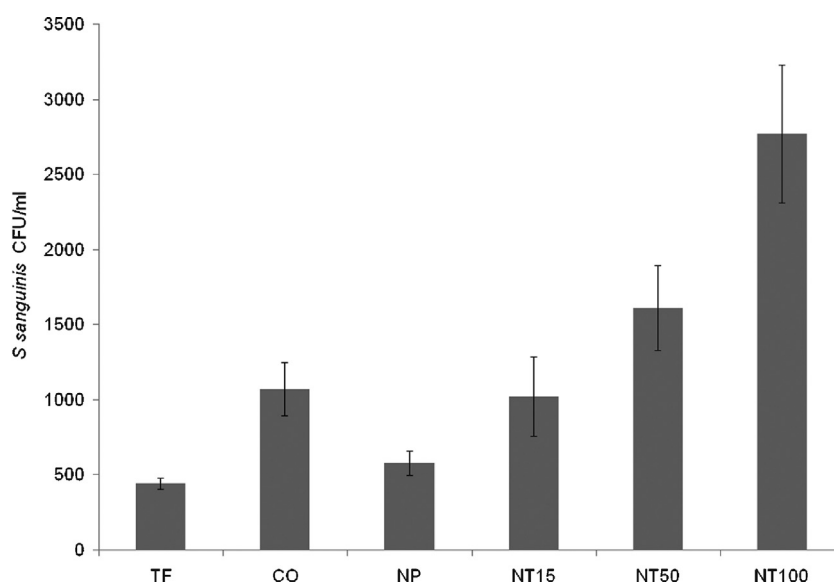


Fig. 5 – Adhesion of *S. sanguinis* (mean CFU/mL) on TiO₂ nanostructures: Ti foil (TF), compact oxide (CO), nanopores (NP), nanotubes (NT). A one-way ANOVA and post-hoc Tukey test ($\alpha = 0.05$) indicated that the NT100 mean was significantly higher than all the others ($P < 0.01$) and NT 50 was significantly higher than NP and TF ($P = < 0.01$). However the difference between NT 50 and NT15 was only just significant ($P = 0.045$). Other pairwise comparisons were not significant.

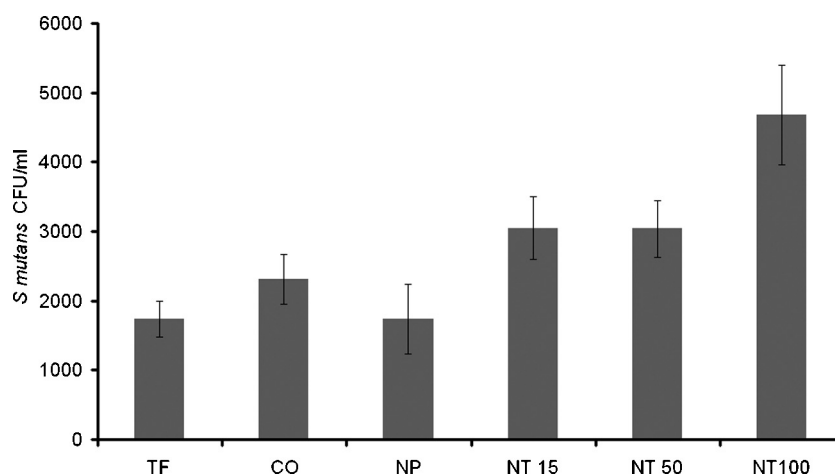


Fig. 6 – Adhesion of *S. mutans* (mean CFU/mL) on TiO₂ nanostructures: Ti foil (TF), compact oxide (CO), nanopores (NP), nanotubes (NT). A one-way ANOVA and post-hoc Tukey tests ($\alpha = 0.05$) identified that there was a significant difference between NT100 and all others but no significant difference between NT15 and NT50 ($P = 1$). NT15, NT50 and CO were not significantly different; nor were CO, NP and TF ($P > 0.05$) but NT15 and NT50 were significantly higher than NP and TF ($P = 0.02$ and $P = 0.01$, respectively).

increase with the fluorine content of the surface [37]. XPS analysis confirmed that the fluoride content of the test surfaces had increased during the anodization process resulting in increasing concentrations in the order NT15 < NT50 < NT100. It may be possible to reduce the fluoride content by annealing at 400 °C [38], in order to better distinguish between topographical and chemical influences. At the moment it is impossible to say whether enhanced adhesion of the streptococci on our 100 nm diameter surfaces was due to tubule diameter (surface geometry) or to increased fluoride (surface chemistry), their effects on protein adsorption or other factors. It is often proposed that surfaces exhibiting increased bacterial attachment offer an increased surface area or surface energy for attachment by increasing cell-surface contact area and providing favorable binding energies [39]. However weak relationships between surface roughness, surface topology and bacterial adhesion are frequently reported [40] and it is suggested that cell membrane distortion, cell shape, membrane stiffness and the ability of bacteria to form chains all influence surface adhesion on patterned surfaces [40,41].

According to Shin et al. [42], nanotube anodization is normally initially accompanied by a decrease in hydrophobicity due to the formation of Ti(OH)₄ which is hydrophilic. However, the initial hydrophilicity may decrease over time due to oxidation in air resulting in the replacement of Ti(OH)₄, by TiO₂, which is hydrophobic and also due to carbon contamination, which occurs after exposing titanium surface to the atmosphere [38,42,43]. Differences in wettability were observed by these authors within days of manufacture with hydrophobicity gradually increasing within a 3 month period. In our study oxidation could well have occurred within the experimental period: Bacterial adherence was tested after 2–4 weeks of sample manufacture and contact angles determined and XPS analysis carried out after approximately 6 weeks. The presence of Ti as TiO₂ (Ti⁴⁺ oxidation state) was confirmed by XPS surface analysis. Other factors that can influence wettability include the height of the nanotubes [44] and surface

roughness, due to entrapment of air [45]. However, in this case we might expect the superior roughness of the NT100 surface, revealed by the AFM images, to result in an increased hydrophobicity in comparison with the smoother surfaces, but the opposite was observed. It is important to note the dynamic nature of nanotubular surfaces for further studies however contact angle will change in the presence of saliva due to protein adsorption [46] and the results of a previous study of streptococcal adherence to composite materials in the presence and absence of salivary proteins suggested that the adsorption of specific proteins that present functional groups to which the bacteria bind may be more relevant for initial bacterial adhesion than hydrophobicity [47].

Although bacterial adherence increased with fluoride this may have beneficial antimicrobial effects over longer time periods since it increases bacterial membrane permeability and inhibits glycolysis [48]. Further work will investigate survival and biofilm formation on the nanotextured surfaces using mixed bacterial cultures including periodontal pathogens and test the “race for the surface” [49] in co-cultures with competing bacteria and mammalian cells.

5. Conclusion

In this study we have shown that adherence of oral streptococci can be modified by changes in nanostructured titanium surface properties such as nanotube diameter and/or fluoride content. From this and previous work we propose that it is possible to tailor the nanostructure to reduce oral bacterial adhesion while enhancing mammalian cell adherence. These preliminary studies highlight the importance of monitoring chemical changes in the surface properties over time but also point the way forward to further studies with these and other bacteria, including pathogens associated with peri-implant diseases, to determine the survival time of bacteria on the surfaces, monitor biofilm formation and assess the adherence

of osteoblasts and oral keratinocytes in cell-bacterial co-cultures. The lowest adhesion of *S. sanguinis* and *S. mutans* on TiO₂ nanostructured surfaces was observed for small diameter nanoporous surfaces (Figs. 5 and 6) – which coincides with the highest osteoblast adhesion on small diameter nanotubular/nanoporous surfaces [31].

Conflict of interest

The authors report no conflicts of interest in this work.

Acknowledgements

The authors wish to acknowledge the Slovenian Research Agency grants (P2-0082 and P2-0232) and the UK EPSRC grant EP/I50124X/1 for financial support. We also thank Dr Virginia Ward, University of Aston, Birmingham, UK, for assistance with the contact angle measurements.

REFERENCES

- [1] Lindhe J, Meyle J. Peri-implant diseases: consensus report of the sixth European workshop on periodontology. *Journal of Clinical Periodontology* 2008;35:282–5.
- [2] Heitz-Mayfield LJA, Lang NP. Comparative biology of chronic and aggressive periodontitis vs peri-implantitis. *Periodontology* 2000 2010;53:167–81.
- [3] Atieh MA, Alsabeeha NHM, Faggion Jr CM, Duncan WJ. The frequency of peri-implant diseases: a systematic review and meta-analysis. *Journal of Periodontology* 2013;84:1586–98.
- [4] Bazaka OKB. Surface modification of biomaterials for biofilm control. In: Barnes L, Cooper I, editors. *Biomaterials and medical device – associated infections*. Woodhead Publishing; 2015. p. 103–12.
- [5] Neoh KG, Wang R, Kang ET. Surface nanoengineering for combating biomaterials infections. In: Barnes L, Cooper I, editors. *Biomaterials and medical device – associated infections*. Woodhead Publishing; 2015. p. 133–61.
- [6] Botos S, Yousef H, Zweig B, Flinton R, Weiner S. The effects of laser microtexturing of the dental implant collar on crestal bone levels and pen-implant health. *International Journal of Oral & Maxillofacial Implants* 2011;26:492–8.
- [7] Ketabi M, Deporter D. The effects of laser microgrooves on hard and soft tissue attachment to implant collar surfaces: a literature review and interpretation. *International Journal of Periodontics & Restorative Dentistry* 2013;33:E145–52.
- [8] Liu X, Zhou X, Li S, Lai R, Zhou Z, Zhang Y, et al. Effects of titania nanotubes with or without bovine serum albumin loaded on human gingival fibroblasts. *International Journal of Nanomedicine* 2014;9:1185–98.
- [9] Applerot G, Lellouche J, Perkas N, Nitzan Y, Gedanken A, Banin E. ZnO nanoparticle-coated surfaces inhibit bacterial biofilm formation and increase antibiotic susceptibility. *RSC Advances* 2012;2:2314–21.
- [10] Ferraris S, Venturello A, Miola M, Cochis A, Rimondini L, Spriano S. Antibacterial and bioactive nanostructured titanium surfaces for bone integration. *Applied Surface Science* 2014;311:279–91.
- [11] Lellouche J, Friedman A, Lahmi R, Gedanken A, Banin E. Antibiofilm surface functionalization of catheters by magnesium fluoride nanoparticles. *International Journal of Nanomedicine* 2012;7:1175–88.
- [12] Kulkarni M, Mazare A, Gongadze E, Perutkova S, Kralj-Iglic V, Milosev I, et al. Titanium nanostructures for biomedical applications. *Nanotechnology* 2015;26:062002.
- [13] Macak JM, Taveira LV, Tsuchiya H, Sirotka K, Schmuki P. Influence of different fluoride containing electrolytes on the formation of self-organized titania nanotubes by Ti anodization. *Journal of Electroceramics* 2006;16:29–34.
- [14] Zwilling V, Darque-Ceretti E, Boutry-Forveille A, David D, Perrin M, Aucouturier M. Structure physicochemistry of anodic oxide films on titanium and TA6V alloy. *Surface and Interface Analysis* 1999;27:629–37.
- [15] Assefpourdezfuly M, Vlachos C, Andrews EH. Oxide morphology adhesive bonding on titanium surfaces. *Journal of Materials Science* 1984;19:3626–39.
- [16] Albu SP, Ghicov A, Macak JM, Schmuki P. 250 μm long anodic TiO₂ nanotubes with hexagonal self-ordering. *Physica Status Solidi (RRL)-Rapid Research Letters* 2007;1:R65–7.
- [17] Wei W, Berger S, Shrestha N, Schmuki P. Ideal hexagonal order: formation of self-organized anodic oxide nanotubes and nanopores on a Ti-35Ta alloy. *Electrochemistry Communications* 2010;157:1184–6.
- [18] Aronsson BO, Lausmaa J, Kasemo B. Glow discharge plasma treatment for surface cleaning and modification of metallic biomaterials. *Journal of Biomedical Materials Research* 1997;35:49–73.
- [19] Kowalski D, Kim D, Schmuki P. TiO₂ nanotubes, nanochannels and mesosponge: self-organized formation and applications. *Nano Today* 2013:235–64.
- [20] Gongadze E, Kabaso D, Bauer S, Slivnik T, Schmuki P, van Rienen U, et al. Adhesion of osteoblasts to a nanorough titanium implant surface. *International Journal of Nanomedicine* 2011;6:1801–16.
- [21] Grigorescu S, Ungureanu C, Kirchgeorg R, Schmuki P, Demetrescu I. Various sized nanotubes on TiZr for antibacterial surfaces. *Applied Surface Science* 2013;270:190–6.
- [22] Peng Z, Ni J, Zheng K, Shen Y, Wang X, He G, et al. Dual effects and mechanism of TiO₂ nanotube arrays in reducing bacterial colonization and enhancing C3H10T1/2 cell adhesion. *International Journal of Nanomedicine* 2013;8:3093–105.
- [23] Gongadze E, Kabaso D, Bauer S, Park J, Schmuki P, Iglic A. Adhesion of osteoblasts to a vertically aligned TiO₂ nanotube surface. *Mini-Reviews in Medicinal Chemistry* 2013;13:194–200.
- [24] Cosyn J, Van Aelst L, Collaert B, Persson GR, De Bruyn H. The peri-implant sulcus compared with internal implant and suprastructure components: a microbiological analysis. *Clinical Implant Dentistry and Related Research* 2009;13:286–95.
- [25] do Nascimento C, Pita MS, Nogueira FH, Fernandes C, Pedrazzi V, de Albuquerque RF, et al. Bacterial adhesion on the titanium and zirconia abutment surfaces. *Clinical Oral Implants Research* 2014;25:337–43.
- [26] Fuerst MM, Salvi GE, Lang NP, Persson GR. Bacterial colonization immediately after installation on oral titanium implants. *Clinical Oral Implants Research* 2007;18:501–8.
- [27] Shibli JA, Melo L, Ferrari DS, Figueiredo LC, Faveri M, Feres M. Composition of supra- and subgingival biofilm of subjects with healthy and diseased implants. *Clinical Oral Implants Research* 2008;19:975–82.
- [28] Pratten J, Smith AW, Wilson M. Response of single species biofilms and microcosm dental plaques to pulsing with chlorhexidine. *Journal of Antimicrobial Chemotherapy* 1998;42:453–9.
- [29] Lee K, Mazare A, Schmuki P. One-dimensional titanium dioxide nanomaterials: nanotubes. *Chemical Reviews* 2014;114:9385–454.

- [30] Teughels W, Van Assche N, Slieden I, Quirynen M. Effect of material characteristics and/or surface topography on biofilm development. *Clinical Oral Implants Research* 2006;17:68–81.
- [31] Ercan B, Taylor E, Alpaslan E, Webster TJ. Diameter of titanium nanotubes influences anti-bacterial efficacy. *Nanotechnology* 2011;22:295102.
- [32] Bauer S, Pittrof A, Tsuchiya H, Schmuki P. Size-effects in TiO₂ nanotubes: diameter dependent anatase/rutile stabilization. *Electrochemistry Communications* 2011;13:538–41.
- [33] Park J, Bauer S, Pittrof A, Killian MS, Schmuki P, von der Mark K. Synergistic control of mesenchymal stem cell differentiation by nanoscale surface geometry and immobilized growth factors on TiO₂ nanotubes. *Small* 2012;8:98–107.
- [34] Park J, Bauer S, Schlegel KA, Neukam FW, von der Mark K, Schmuki P. TiO₂ nanotube surfaces: 15 nm – an optimal length scale of surface topography for cell adhesion and differentiation. *Small* 2009;5:666–71.
- [35] Puckett SD, Taylor E, Raimondo T, Webster TJ. The relationship between the nanostructure of titanium surfaces and bacterial attachment. *Biomaterials* 2010;31:706–13.
- [36] Kulkarni M, Flasker A, Lokar M, Mrak-Poljsak K, Mazare A, Artenjak A, et al. Binding of plasma proteins to titanium dioxide nanotubes with different diameters. *International Journal of Nanomedicine* 2015;10:1359–73.
- [37] Katsikogianni M, Spiliopoulou I, Dowling D, Missirlis YJ. Adhesion of slime producing *Staphylococcus epidermidis* strains to PVC and diamond-like carbon/silver/fluorinated coatings. *Journal of Materials Science: Materials in Medicine* 2006;17:679–89.
- [38] Regonini D, Jaroenworarluck A, Stevens R, Bowen CR. Effect of heat treatment on the properties and structure of TiO₂ nanotubes: phase composition and chemical composition. *Surface and Interface Analysis* 2010;42:139–44.
- [39] Scheuerman TR, Camper AK, Hamilton MA. Effects of substratum topography on bacterial adhesion. *Journal of Colloid and Interface Science* 1998;208:23–33.
- [40] Anselme K, Davidson P, Popa AM, Giazzon M, Liley M, Ploux L. The interaction of cells and bacteria with surfaces structured at the nanometre scale. *Acta Biomaterialia* 2010;6(October (10)):3824–46.
- [41] Medilanski E, Kaufmann K, Wick LY, Wanner O, Harms H. Influence of the surface topography of stainless steel on bacterial adhesion. *Biofouling* 2002;18:193–203.
- [42] Shin DH, Shokuhfar T, Choi CK, Lee S-H, Friedrich C. Wettability changes of TiO₂ nanotube surfaces. *Nanotechnology* 2011;22:315704.
- [43] Zhu XL, Chen J, Scheideler L, Reichl R, Geis-Gerstorfer J. Effects of topography and composition of titanium surface oxides on osteoblast responses. *Biomaterials* 2004;25:4087–103.
- [44] Quere D. Surface chemistry: Fakir droplets. *Nature Materials* 2002;1:14–5.
- [45] Herminghaus S. Roughness-induced non-wetting. *Europhysics Letters* 2000;52:165–70.
- [46] Satou J, Fukunaga A, Morikawa A, Matsumae I, Satou N, Shintani H. Streptococcal adherence to uncoated and saliva-coated restoratives. *Journal of Oral Rehabilitation* 1991;18:421–9.
- [47] Schweickl H, Hiller K-A, Carl U, Schweiger R, Eidt A, Ruhl S, et al. Salivary protein adsorption and *Streptococcus gordonii* adhesion to dental material surfaces. *Dental Materials* 2013;29:1080–9.
- [48] Marquis RE. Antimicrobial actions of fluoride for oral bacteria. *Canadian Journal of Microbiology* 1995;41: 955–64.
- [49] Gristina AG. Biomaterial-centred infection: microbial adhesion versus tissue integration. *Science* 1987;237: 1588–9.